Journal of Earthquake Engineering

SEISMIC HAZARD IN THE ISTANBUL METROPOLITAN AREA: A PRELIMINARY RE-EVALUATION

E. KALKAN [a], P. GÜLKAN [b], N. YILMAZ ÖZTÜRK [c] and M. ÇELEBİ [d]

Received (Sept. 2007)
Revised (Dec. 2007)
Accepted (Jan. 2008)

Seismic activity on the western extension of the North Anatolian Fault (NAF) system has increased during the last decade with two destructive events in 1999 (M7.4 Kocaeli and M7.2 Düzce). These earthquakes resulted in major stress-drops on the western segment of the NAF where it extends under the Marmara Sea. These undersea fault segments were recently explored using bathymetric and reflection surveys. These recent findings helped to reshape the seismotectonic environment of the Marmara basin which is a perplexing tectonic domain. Based on collected new information, seismic hazard of the Marmara region, particularly Istanbul Metropolitan Area and its vicinity were re-examined using a probabilistic approach. Alternate seismic source and magnitude-frequency relations combined with various indigenous and "foreign" attenuation relationships were adapted within a logic tree formulation to quantify and project the regional exposure on a set of hazard maps. The hazard maps show the peak horizontal ground acceleration and spectral acceleration at 1.0 sec. These acceleration levels were computed for 2 and 10 percent probabilities of being exceeded in 50 years.

Keywords: Sea of Marmara region, probabilistic seismic hazard, ground motion prediction

INTRODUCTION

The Marmara Sea region housing one third of Turkey population is one of the most tectonically active regions in Eurasia. In the last century, this region witnessed unusual seismic activities with nine district events having M>7.0 (M stands for moment magnitude). In 1999, two destructive earthquakes (Kocaeli and Duzce) occurred in the eastern part of the Marmara region on the NAF system. This strike-slip fault system cuts across northern Turkey for more than 1500 km, and accommodates ~25 mm/year right-lateral slip between Anatolia and Eurasian plate (Straub et al., 1997; McClusky et al., 2000). Based on the renewal model, the probability of occurrence of M7.0 and greater earthquakes in the Marmara Sea region (which would directly affect the Istanbul Metropolitan area) was computed as 44±18 percent in the next 30 years (Parsons, 2004). As implied by the level of hazard exposure in the Marmara region, and especially in the

[a] Earthquake Engineering Program, California Geological Survey, Sacramento, CA 95814, USA.
[b] Department of Civil Engineering, Middle East Technical University, Ankara 06531, Turkey.
[c] Earthquake Research Department, General Directorate of Disaster Affair, Ankara, Turkey.
[d] USGS, Western Region Earthquake Hazards Team, Menlo Park, CA 94025, USA.

Istanbul Metropolitan area due to its socio-economic importance, critical assessment of the regional seismic hazard retains paramount priority for preparedness and other regional earthquake engineering applications. This paper is a summary of a longer article that will examine other current assessments of the seismic hazard in the region.

REGIONAL SEISMICITY AND TECTONIC SETTING

The Marmara Sea region, limited in this study to within latitudes 39-43 deg. N and longitudes 26-32 deg. E, is one of the most seismically active regions of the continent as manifested by the number of large earthquakes (M ≥ 6.0) that occurred during 1509-1999. The epicenters of these events are depicted in Figure 1. Many of these events ruptured on or in proximity of the NAF system. A moderate to large earthquakes with M ≥ 6.0 also occurred on fault segments situated well away from the NAF. For regional seismic hazard formulation, all potential sources of seismic activity that could produce significant ground motions were identified and characterized based on geologic, tectonic, historical and instrumental evidences. Two major ingredients of hazard computation that follow are the earthquake catalog and fault segmentation data.

The current regulatory seismic zoning map in Turkey including the Marmara Sea region is based on a study (Gülkan et al., 1993) using then available earthquake catalog and attenuation expressions originally developed for western U.S. ground motion data. In the past 14 years, a large number of additional strong motion records were obtained in Turkey, which has allowed development of regional attenuation relationships (Gülkan and Kalkan, 2002; Kalkan and Gülkan, 2004a,b; Ulusay et al., 2004). In addition, tracing of new fault segments beneath the Marmara Sea augments our understanding of the seismotectonic environment of the Marmara basin (e.g., Le Pichon et al., 2001; Armijo et al., 2002).

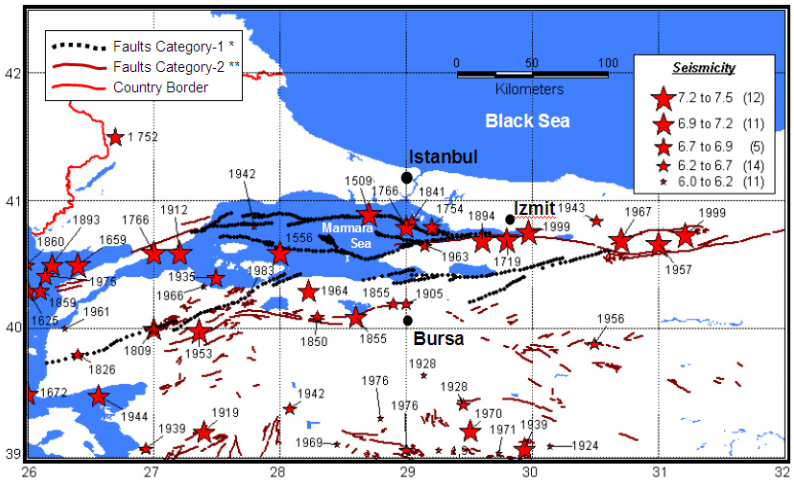

Fig. 1. Locations of **M** ≥ 6.0 earthquakes (A.D. 1509-1999) (Note: Parentheses in the legend denote the breakdown of earthquakes; Category-1 faults were recently visualized using bathymetric images and seismic reflection survey; Category-2 faults indicate the previously known faults).

The regional seismic catalog integrates both historical and instrumental seismicity of the region. Historical accounts of earthquakes can be used to confirm the occurrence of past events and to predict geographic distributions of intensity. Historical events are only complete between M6.0 and M8.0 for about 400 years (A.D. 1509-1900). The epicenter coordinates of all events with M ≥ 6.0 (both from historical and instrumental seismicity) and their depths are presented in Table 1. For historical events, conversion to moment magnitude was made from empirical relations.

Table 1. Major earthquakes in the Marmara Sea region (M ≥ 6.0, A.D. 1509-1999)

No.	Year	Month	Day	Latitude	Long.	Depth (km)	Mw	Approx. Rupture Length (km)*	Source**
1	1509	9	10	40.900	28.700	-	6.7	24	1
2	1556	5	10	40.600	28.000	-	6.7	24	2
3	**1625**	5	18	40.300	26.000	-	**7.1**	54	2
4	**1659**	2	17	40.500	26.400	-	**7.2**	66	2
5	**1672**	2	14	39.500	26.000		**7.0**	44	2
6	1719	5	25	40.700	29.800	-	6.8	29	2
7	1737	3	6	40.000	27.000	-	6.6	19	2
8	1752	7	29	41.500	26.700		6.8	29	2
9	1754	9	2	40.800	29.200	-	6.5	15	2
10	1766	5	22	40.800	29.000	-	6.6	21	2
11	1766	8	5	40.600	27.000	-	6.8	29	2
12	1826	2	8	39.800	26.400	-	6.2	8	1
13	1841	10	6	40.850	29.050	-	6.1	7	1
14	1850	4	19	40.100	28.300	-	6.1	7	1
15	1855	2	28	40.100	28.600	-	6.6	21	2
16	1855	4	11	40.200	28.900	-	6.2	9	1
17	1859	8	21	40.300	26.100	-	6.5	15	2
18	1860	8	22	40.500	26.000	-	6.1	7	1
19	1893	2	9	40.500	26.200	-	6.5	17	2
20	1894	7	10	40.700	29.600	-	6.8	26	2
21	1905	4	15	40.200	29.000		6.6	19	6
22	**1912**	8	10	40.600	27.200	16	**7.4**	100	6
23	**1919**	11	18	39.200	27.400	-	**7.0**	44	3
24	1924	11	20	39.080	30.140	-	6.0	6	4
25	1928	5	2	39.410	29.450	-	6.2	8	4
26	1928	5	3	39.640	29.140	10	6.1	7	6
27	1935	1	4	40.400	27.490	30	6.7	24	6
28	**1939**	9	22	39.070	29.940	10	**7.1**	54	6
29	1939	10	19	39.070	26.940	10	6.6	19	6
30	1942	6	16	40.800	27.800	20	6.0	6	6
31	1942	11	15	39.380	28.080	-	6.2	8	4
32	1943	6	20	40.850	30.510	10	6.6	19	6
33	1944	6	25	39.050	29.260	-	6.1	7	3
34	**1944**	10	6	39.480	26.560	40	**7.0**	44	6
35	**1953**	3	18	39.990	27.360	10	**7.5**	123	6
36	1956	2	20	39.890	30.490	40	6.4	13	6
37	1957	5	26	40.670	31.000	10	**7.2**	66	6
38	1961	11	28	40.000	26.300	120	6.0	6	6
39	1963	9	18	40.650	29.150	-	6.4	13	4
40	1964	10	6	40.300	28.230	34	6.9	36	3
41	1966	8	21	40.330	27.400	12	6.0	6	6
42	1967	7	22	40.700	30.700	-	**7.2**	66	1
43	1969	3	25	39.100	28.450	-	6.1	7	4
44	1970	3	28	39.210	29.510	18	**7.1**	54	3
45	1971	5	25	39.027	29.737	24	6.1	7	5
46	1975	3	27	40.418	26.139	5	6.7	24	5
47	1976	8	25	39.300	28.800	33	6.0	6	6
48	1976	9	6	39.060	29.000	11	6.6	19	6
49	1983	7	5	40.280	27.760	-	6.1	7	1
50	**1999**	8	17	40.760	29.970	18	**7.4**	100	7
51	**1999**	11	12	40.740	31.210	25	**7.2**	66	7

** Based on Wells and Coppersmith (1994) empirical formulations.*
*** Sources: [1] Ambraseys and Jackson (2000); [2] Ambraseys (2002); [3] Papazachos and Papazachou (1997); [4] Ambraseys and Moinfar (1988); [5] CNSS Catalogue U.S. Council of National Seismic System; [6] KOERI; [7] Gulkan and Kalkan (2002)*

The Marmara Sea region has very complex and heterogeneous fault system as depicted by the regional seismotectonics in Figure 1. The 1500 km long NAF fault system extends from the east of the region. NAF system in the east at the junction of the Marmara Sea is controlled by right-lateral dextral strike-slip faults, while the plate boundary changes into a trans-tensional system that has opened deep-basin beneath the Marmara Sea. There is no evidence of a single, continuous, purely strike-slip fault under the sea (Le Pichon et al., 2001), but a complex segmented fault system with large normal components identified based on seismic reflection surveys (e.g., Smith et al., 1995; Okay et al., 2000; Parke et al., 2000). These findings are crucial for understanding the tectonic behavior of the region of the NAF zone. A series of strong earthquakes broke the NAF zone, Kocaeli and Düzce events were the latest among successive westerly propagating earthquake sequence on this fault system which began with the magnitude 7.9 Erzincan earthquake in the eastern part of Turkey in 1939, and has generated nine more destructive earthquakes (similar to topping of domino pieces) with magnitudes greater than 7 since. This earthquake sequence is illustrated in Figure 2. The 1912 event occurred in the west of the Sea of Marmara but there is a seismic gap, still in effect, that crosses the northern border of the sea (Barka, 1992; Stein et al., 1997). According to Ambraseys and Jackson (2000), the seismicity of the last 500 years in the Marmara region can account for most of the expected 22±3 mm per year right-lateral slip. While we assigned 23 mm slip-rate to

major faults passing underneath of the Marmara Sea, for the rest of the fault segments, we used the slip-rate distribution of Straub et al. (1997) based on GPS measurements. The measured slip vectors in the Anatolian Plate with respect to stable Eurasia exhibit a general anticlockwise rotation, and an increase in total displacement towards the west caused by the westward increasing pull of the Hellenic subduction system located western south of Turkey (McClusky et al., 2000). This dynamism pushes the Marmara region in north direction. The slip-rate distributions agree with recent tectonic studies reported (e.g., Motagh et al., 2007; Seeber et al., 2004; Pulido et al., 2004; Yaltirak, 2002; McClusky et al., 2000; Barka and Kadinsky-Cade, 1988). The complete list of slip-rates for each fault included in hazard computation is given in Table 2. Also in this table are the major characteristic attributes of the faults.

Table 2. Characteristic attributes of the Marmara Sea region fault segmentation model

Fault Segment	Style of Faulting *	Length (km)	Characteristic Event (M)	Slip-Rate (mm/yr) *	Activity Rate (Eqk/yr)	Fault Segment	Style of Faulting *	Length (km)	Characteristic Event (M)	Slip-Rate (mm/yr) *	Activity Rate (Eqk/yr)
F1	Strike-Slip	45	7.0	20	0.0073	F25	Strike-Slip	31	6.8	20	0.0095
F2	Strike-Slip	48	7.0	20	0.0070	F26	Strike-Slip	44	7.0	20	0.0074
F3	Strike-Slip	82	7.3	20	0.0049	F27	Strike-Slip	42	7.0	20	0.0077
F4	Strike-Slip	31	6.8	20	0.0094	F28	Strike-Slip	51	7.1	23	0.0077
F5	Strike-Slip	36	6.9	20	0.0085	F29	Strike-Slip	62	7.2	23	0.0068
F6	Strike-Slip	22	6.7	20	0.0119	F30	Strike-Slip	51	7.1	23	0.0077
F7	Strike-Slip	28	6.8	20	0.0101	F31	Strike-Slip	20	6.6	23	0.0148
F8	Strike-Slip	63	7.2	20	0.0058	F32	Strike-Slip	16	6.5	20	0.0150
F9	Strike-Slip	58	7.1	20	0.0062	F33	Strike-Slip	57	7.1	20	0.0062
F10	Strike-Slip	40	7.0	20	0.0079	F34	Strike-Slip	20	6.6	20	0.0128
F11	Strike-Slip	28	6.8	20	0.0101	F35	Strike-Slip	41	7.0	20	0.0077
F12	Strike-Slip	46	7.0	20	0.0072	F36	Strike-Slip	36	6.9	20	0.0085
F13	Strike-Slip	21	6.6	20	0.0121	F37	Strike-Slip	112	**7.5**	23	0.0045
F14	Strike-Slip	29	6.8	20	0.0099	F38	Normal	36	6.9	18	0.0076
F15	Strike-Slip	21	6.7	20	0.0121	F39	Strike-Slip	15	6.5	18	0.0140
F16	Strike-Slip	66	7.2	20	0.0056	F40	Normal	37	6.9	18	0.0075
F17	Strike-Slip	21	6.6	20	0.0122	F41	Normal	30	6.8	18	0.0088
F18	Strike-Slip	21	6.6	20	0.0124	F42	Normal	10	6.3	18	0.0185
F19	Strike-Slip	90	7.3	20	0.0046	F43	Strike-Slip	20	6.6	15	0.0096
F20	Strike-Slip	26	6.7	20	0.0107	F44	Strike-Slip	22	6.7	15	0.0089
F21	Thrust	19	6.6	20	0.0133	F45	Strike-Slip	15	6.5	15	0.0116
F22	Thrust	23	6.7	20	0.0114	F46	Strike-Slip	20	6.6	15	0.0096
F23	Normal	49	7.1	10	0.0034	F47	Strike-Slip	30	6.8	20	0.0097
F24	Normal	33	6.9	10	0.0045	F48	Strike-Slip	46	7.0	20	0.0072

* Data is compiled by searching most reliable literature sources, despite that it may show variations from one source to other.

METHODOLOGY

Our approach in computing the regional seismic hazard constitutes two different seismicity models similar to those used in development of the regulatory USGS National Seismic Hazard Maps (e.g., Frankel et al., 2002) except that the areal source model was not employed here. These are (i) spatially smoothed seismicity model to account for background seismic activities and their influence on regional seismic hazard, and (ii) segmented fault source model based on distinct seismogenic sources. The smoothed seismicity model addresses the aleatoric uncertainty in location of future earthquakes, thus allows for a spatial stationary of seismicity while eliminating the subjectivity in delineation of aerial sources. In this model, events that are not assigned to specific faults are assumed to be potential seismogenic sources and spatially gridded to cells. For the computation of spatially smoothed seismicity, a catalog having discrete independent earthquakes of $4.0 \leq M \leq 6.5$ was associated to Gutenberg-Richter (GR) magnitude-frequency relation, and $M > 6.5$ events were assigned to segmented fault source model. In general, a total of 48 fault segments were integrated with alternative magnitude-frequency relation and ground motion prediction models. All combinations are treated

within a logic-tree formulation as schematically illustrated in Figure 3. The logic tree combines a total of 8 branches. A recent attenuation relationship (Kalkan and Gülkan, 2004b) specifically developed for shallow crustal tectonic environment of the Turkey is used together with a series of ground motion prediction equations developed for California (Abrahamson and Silva, 1997; Boore et al., 1997 and Sadigh et al., 1997).

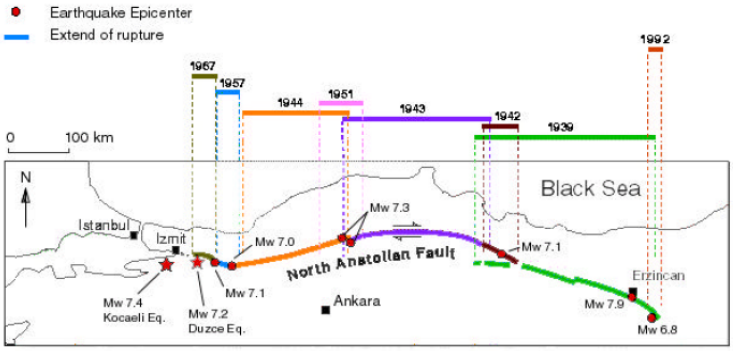

Fig. 2. Westerly propagating successive earthquake sequence on the North Anatolian Fault since 1939 (modified from the USGS website).

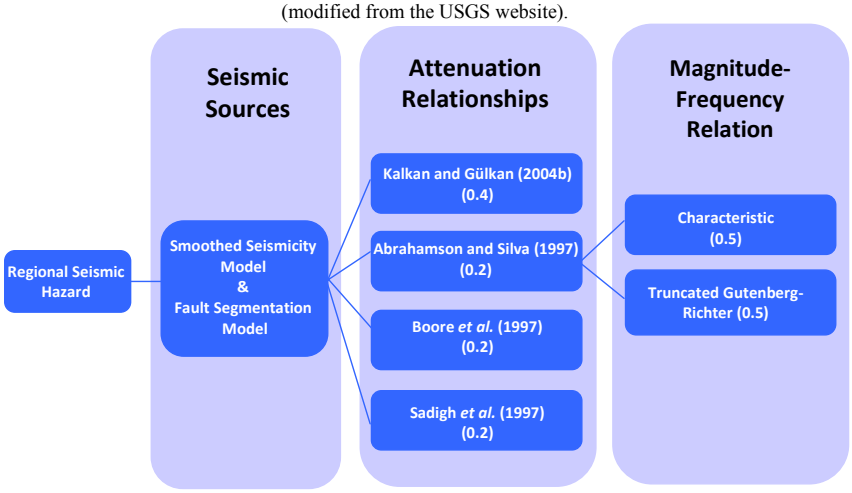

Fig. 3. Logic-tree formalism adapted for probabilistic seismic hazard analysis (Values in parentheses indicate the assigned weight for each cell).

In order to utilize the contribution of the fault sources to regional seismic hazard, four aspects of each source were examined. These are: (a) style-of-faulting; (b) location and orientation; (c) slip-rate; (d) maximum magnitude earthquake expected from the fault (Petersen et al., 2000). For the faults beneath the Marmara Sea, we used fault segmentation data from Le Pichon et al. (2001) and Armijo et al. (2002), which relies on recent bathymetric and seismic reflection surveys. The rest of the faults were retrieved from the active fault map of Turkey (Saroglu et al., 1992). In general, region has a very complex fault system especially within the boundaries of the Marmara Sea. All these fault systems are examined within 48 segments. This segmentation model is depicted in

Figure 4 with the initials marked on each segment, and Table 2 lists their general characteristics. In interpretation of segmentation model, it is instructive to emphasize that geometry and magnitude-frequency relation are not totally independent from each other. For instance, if a fault is modeled with several small segments instead of fewer large segments, the maximum magnitude will be lower, and a given slip-rate will require many more small earthquakes to accommodate a cumulative seismic moment.

For segmented faults source model, historical and instrumented data available is not sufficient enough to determine whether the GR model or characteristic earthquake (CE) model or some other magnitude-frequency relation (e.g., hybrid model of Youngs and Coppersmith, 1985) is more appropriate. Therefore, two different models (GR and CE) were adapted within the logic tree to determine the rate of earthquakes.

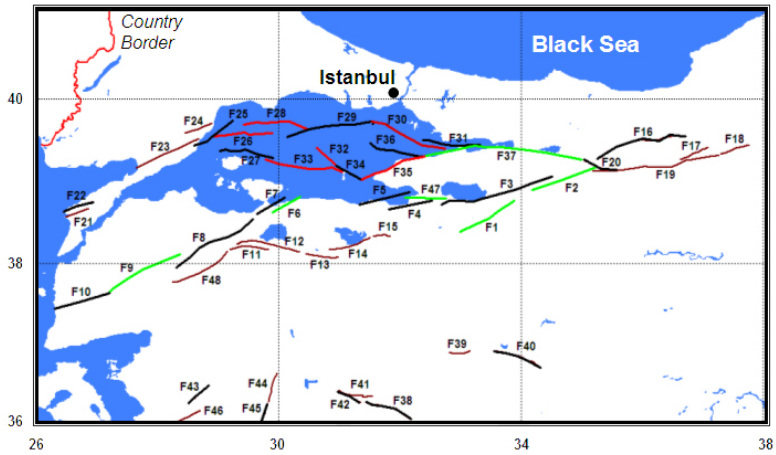

Fig. 4. Fault segmentation model for the Marmara Sea region.

For the faults whose slip-rate data is available, we used the following seismic moment formulation to find the activity rate of the characteristic event

$$M_0 = \mu AD \tag{3.1}$$

where M_0 is the seismic moment of the characteristic earthquake. Time derivative of Eq. (3.1) results in a moment rate as a function of slip-rate.

$$M_0' = \mu AS \tag{3.2}$$

where M_0' is the moment rate and S is the slip-rate. Note that seismic moment can be obtained through M based on the relation given by Hanks and Kanamori (1979) as:

$$M = 2/3 \log M_0 - 10.7 \tag{3.3}$$

By manipulating Eq. (3.3), the activity rate of earthquakes above a minimum magnitude, M_{min}, can be found as

$$N(M_{\min}) = \frac{\mu AS}{mean(M_0 / earthquake)} \tag{3.4}$$

Truncated GR model on the hand requires computation of "a" values (incremental rate) for the fault segments. We used regional "b" value of 0.58 based on complete GR-model to compute the corresponding "a" values for each fault. Buffer zones with radius of 10-15 km were introduced around the faults, and events within each confined zone were counted. If one event was counted for one buffer zone, it was not included in another zone although it might fall into radius of other zone(s). A line equation was fitted in log-space to number of earthquake data distributed with respect to their magnitudes to compute the "a" values. To avoid double counting considering the smoothed seismicity model, minimum magnitude of GR model is set to 6.5 (although all the events were considered in computation of "a" values). The final parameters of both GR and CE models for each active fault segment in the Marmara Sea region were also projected in Table 2. As a recurrence forecasting process, Poisson model was employed for both GR and CE models to estimate the probability of being exceeded in finite time interval. While the Poisson model assumes an independence of events that is inconsistent with elastic rebound theory, it remains the most commonly employed model in PSH analyses.

HAZARD MAPS

Regional seismic hazard maps in terms of peak horizontal ground acceleration (PGA) and spectral acceleration at 1.0 sec with 2 and 10 percent probability of being exceeded (PE) in 50 years created for generic rock site condition ($V_{S30} \cong 760$ m/sec). Figures 5 and 6 show the median seismic hazard (50th-percentile) for PGA and spectral acceleration at 1.0 sec with 2 and 10 percent probability of being transcended in 50 years corresponding to 4.04×10^{-4} and 2.1×10^{-3} annual rate of being exceeded, respectively. These probabilities are the reciprocal of the average return periods. As obvious, the value of ground motion parameter with a particular exposure time increases with decreasing probability of being exceeded. For 2475 year return period, maximum PGA in the region is predicted as 1.5g in proximity of Izmit segment of NAF, while it diminishes to 0.97 as the return period is reduced to 475 years.

A close-up view to seismic hazard in the vicinity of Istanbul Metropolitan is given next in Figure 7. Notably, this intensity level is expected in southern part of Istanbul where Bosphorus opens into the Marmara Sea. The level of shaking becomes menace in case of 475 year event for which maximum predicted PGA ranges between 0.3 and 0.4g. In the interest of space, we refrain from displaying additional maps of this sort.

CONCLUSIONS

This abbreviated paper contains a concatenated description for a preliminary re-evaluation of the seismic hazard in the Sea of Marmara region. The principal differences of the study described here are that the ground motion prediction equation developed from indigenous sources has been given preponderance in the weighting. The characteristics attributed to the seismogenic sources as well as the wider area investigated are improvements over similar studies that have been reported recently (e.g., Erdik et al., 2004). In this form, the ground motion prediction results reported here represent a more reliable basis for regional risk estimation and disaster planning.

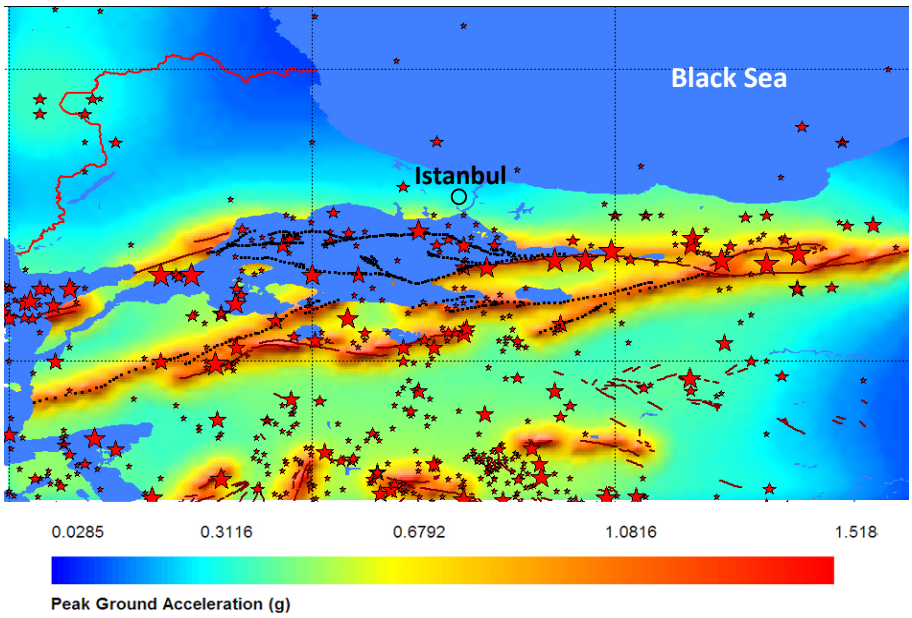

(a)

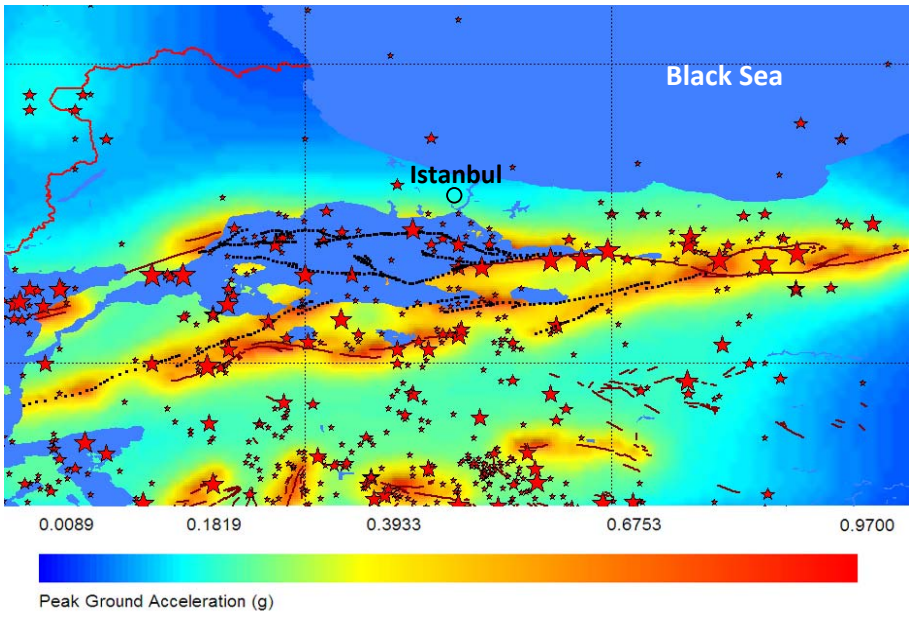

(b)

Fig. 5. Seismic hazard map of the Marmara Sea region for PGA having (a) 2 and (b) 10 percent probability of transcendence in 50 years.

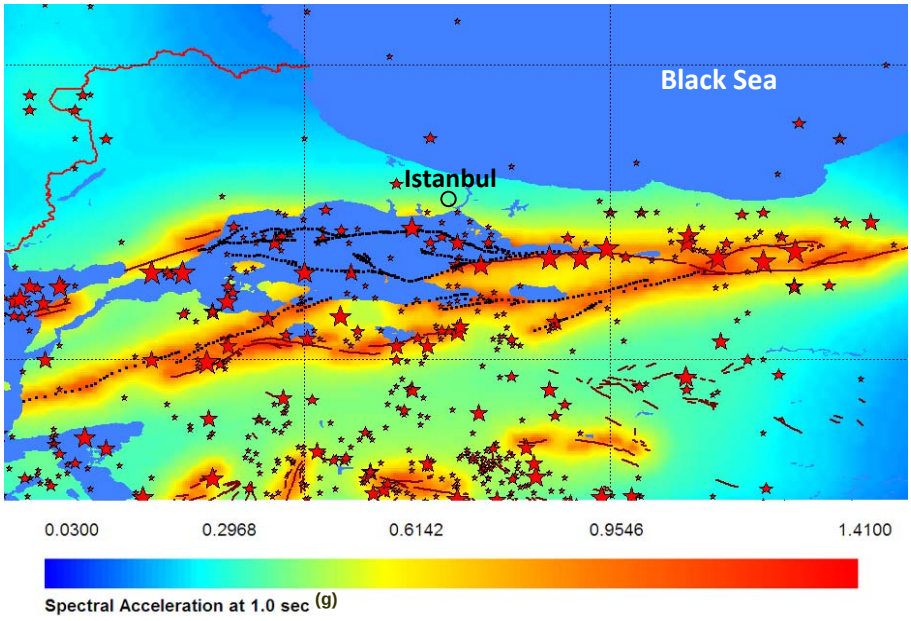

(a)

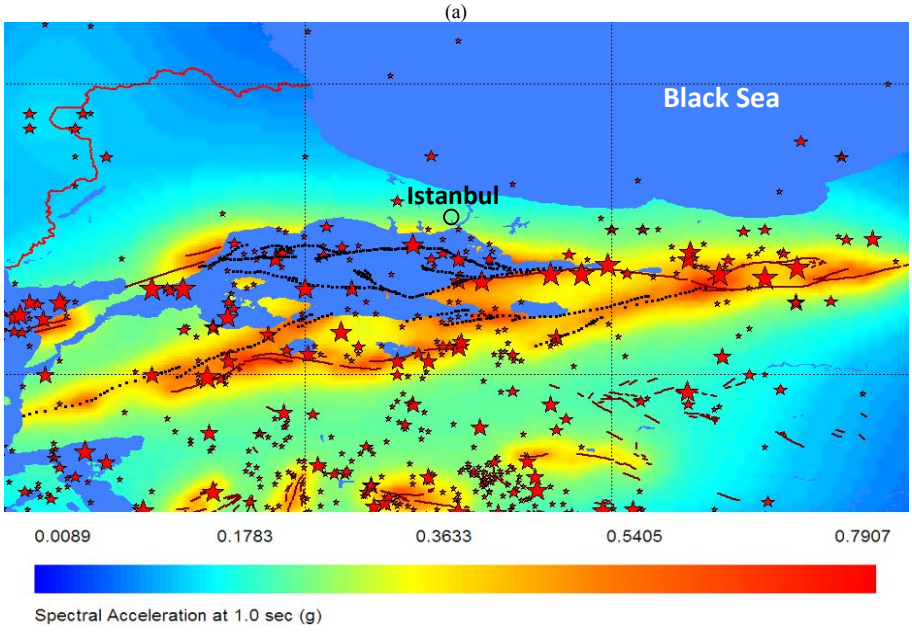

(b)

Fig. 6. Seismic hazard map of the Marmara Sea region for spectral period of 1.0 sec having (a) 2 and (b) 10 percent probability of transcendence in 50 years.

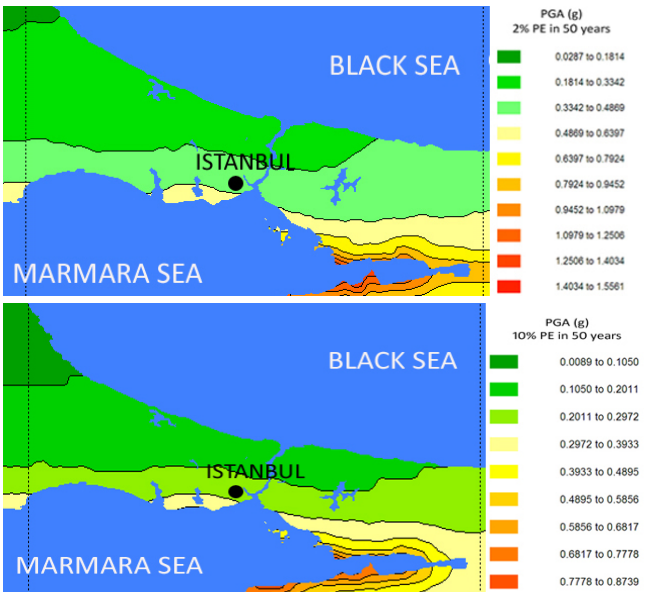

Fig. 7. Contour maps of predicted seismic hazard in the vicinity of Istanbul Metropolitan.

ACKNOWLEDGMENTS

We would like to thank Dr. T. Parsons for generously providing us the coordinates of faults passing under the Marmara Sea. Special thanks are extended to Dr. V. Graizer and Dr. T. Cao for their insightful reviews. Any opinions, findings, and conclusions or recommendations expressed in this article are those of the authors solely and do not necessarily reflect the views of the authors' institutions.

REFERENCES

Ambraseys, N.N. and Moinfar, A.A. (1988). "Isoseismal maps across national frontiers: the Caldiran (Turkey) earthquake of 24 November, 1976", *European Earthquake Engineering*, 1, 15-21.

Ambraseys, N.N. and Jackson, J.A. (2000) "Seismicity of the Sea of Marmara (Turkey) since 1500", *Geophysical Journal International,*141, F1-F6.

Ambraseys, N.N. (2002). "The Seismic Activity of the Marmara Sea Region over the Last 2000 years", *Bulletin of the Seismological Society of America*, 92(1), 1-18.

Armijo, R., Meyer, B., Navarro, S., King, G. and Barka, A. (2002) "Asymmetric slip partitioning in the Sea of Marmara pull-apart: a clue to propagation processes of the North Anatolian Fault?", *Terranova,* 14, 80-86.

Barka, A. and Kadinsky-Cade, K. (1988) "Strike-slip fault geometry in Turkey and its influence on earthquake activity", *Tectonics,* 7(3), 663-684.

Barka, A. (1992). "The North Anatolian fault zone", *Annales Tectonicae*, 6, 164-195.

Boore, D.M., Joyner, W.B. and Fumal, T.E. (1997) "Equations for estimating horizontal response spectra and peak acceleration from Western North American earthquakes: a summary of recent work", *Seismological Research Letters,* 68(1), 128-153.

Erdik, M., Demircioğlu, M., Şeşetyan, K., Durukal, E. and Siyahi, B. (2004) "Earthquake hazard in Marmara region, Turkey", *Soil Dynamics and Earthquake Engineering,* 24, 605-631.

Frankel, A.D., Petersen, M.D., Mueller, C.S., Haller, K.M., Wheeler, R.L., Leyendecker, E.V., Wesson, R.L., Harmsen, S.C., Cramer, C.H., Perkins, D.M., Rukstales, K.S. (2002) "Documentation for the 2002 update of the national seismic hazard maps", *USGS Open-File Report*, 02-420.

Gülkan, P., Koçyiğit, A., Yücemen, M. S., Doyuran, V., Başöz, N. (1993) "En son verilere göre hazırlanan Türkiye deprem bölgeleri haritası," Orta Doğu Teknik Üniversitesi, Deprem Mühendisliği Araştırma Merkezi, Rapor No. 93-01. (in-Turkish)

Gülkan, P. and Kalkan, E. (2002) "Attenuation modeling of recent earthquakes in Turkey," *Journal of Seismology,* 6(3), 397-409.

Hanks, T.C. and Kanamori, H. (1979) "A moment magnitude scale", *Journal of Geophysical Research,* 84, 2348-2350.

Kalkan, E. and Gülkan, P. (2004a) "Empirical attenuation equations for vertical ground motion in Turkey", *Earthquake Spectra,* 20(3), 853-882.

Kalkan, E. and Gülkan, P. (2004b) "Site-dependent spectra derived from ground motion records in Turkey", *Earthquake Spectra,* 20(4), 1111-1138.

Le Pichon, X., Sengor, A.M.C., Demirbag, E., Rangin, C., Imren, C., Armijo, R., Gorur, N., Cagatay, N., Mercier de Lepinay, B., Meyer, B., Saatcilar, R. and Tok, B. (2001) "The active main Marmara fault," *Earth and Planetary Science Letters,* 192, 595-616.

McClusky, S. and 27 coauthors, (2000). "Global Positioning System constraints on plate kinematics and dynamics in the eastern Mediterranean and Caucasus," *Journal of Geophysical Research,* 105, 5695-5719.

Motagh, M., Hoffmann, J., Kampes, B., Baes, M. and Zschau, J. (2007) "Strain accumulation across the Gazikoy–Saros segment of the North Anatolian Fault inferred from Persistent Scatterer Interferometry and GPS measurements", *Earth and Planetary Science Letters,* 255(30), 432-444.

Okay, A.I., Ozcan, A.K., Imren, C., Guney, A.B., Demirbag, E. and Kuscu I. (2000) "Active faults and evolving strike-slip basins in the Marmara Sea, northwest Turkey: a multichannel seismic reflection study", *Tectonophysics,* 321, 189-218.

Papazachos, B.C. and Papazachou, C. 1997. "The Earthquakes of Greece". ZITI editions, Thessaloniki.

Parke, J.R. et al. (1999). "Active faults in the Sea of Marmara, western Turkey, imaged by seismic reflection profiles", *Terra Nova,* 11, 223-227.

Parsons, T. (2004) "Recalculated probability of $M \geq 7$ earthquakes beneath the Sea of Marmara, Turkey", *Journal of Geophysical Research,* 109.

Petersen, M.D., Toppozada, T.R., Cao, T., Cramer, C.H., Reichle, M.S. and Bryant, W.A. (2000) "Active fault near-source zones within and bordering the State of California for the 1997 Uniform Building Code", *Earthquake Spectra,* 16(1), 69-83.

Pulido, N., Ojeda, A., Atakan, K. and Kubo, T. (2004) "Strong ground motion estimation in the Sea of Marmara region (Turkey) based on scenario earthquake", *Tectonophysics,* 39, 357-374.

Saroglu, F., Emre, O. and Kuscu, I. (1992) "Active fault map of Turkey", MTA, Turkey.

Seeber, L., Emre, O., Cormier, M.H., Sorlien, C.C, McHugh, C.M.G., Polonia, A., Ozer, N., Cagatay, N and The team of the 2000 R/V Urania Cruise in the Marmara Sea, (2004). "Uplift and subsidence from oblique slip: the Ganos Marmara bend of the North Anatolian Transform, western Turkey", *Tectonophysics,* 391(1-4), 239-258.

Smith, A.D., Taymaz, T., Oktay, F., Yuce, H., Alpar, B., Basaran, H., Jackson, J.A., Kara, S. and Simsek, M. (1995). "High-resolution seismic profiling in the Sea of Marmara (Northwest Turkey); late Quaternary sedimentation and sea-level changes", *Geological Society of America Bulletin,* 107, 923-936.

Stein, R.S., Barka, A.A. and Dieterich, J.H. (1997). "Progressive failure on North Anatolian Fault since 1939 by earthquake stress triggering". *Geophysical Journal International,* 128, 594-604.

Straub, C., Kahle, H-G., Schindler, C. (1997). "GPS and geologic estimates of the tectonic activity in the Marmara Sea region, NW Anatolia". *Journal of Geophysical Research.* 102(27), 587-601.

Ulusay, R. Tuncay, E., Sonmez, H. and Gokceoglu, C. (2004). "An attenuation relationship based on Turkish strong motion data and iso-acceleration map of Turkey", *Engineering Geology*, 74(3–4), 265–291.

Wells, D.L. and Coppersmith, K.J. (1994). "New empirical relationships among magnitude, rupture length, rupture width, rupture area, and surface displacement", *Bulletin of the Seismological Society of America,* 84(4), 974-1002.

Yaltirak, C. (2002). "Tectonic evolution of the Marmara Sea and its surroundings", *Marine Geology,* 190**,** 493-529.

Yaltirak, C. (2003). "Historical earthquakes of the Marmara Sea: their locations, magnitudes, influence area and activity rates", *Quaternary Workshop*, Istanbul Technical University.

Youngs, R.R. and Coppersmith, K.J. (1985). "Implications of fault slip rates and earthquake recurrence models to probabilistic seismic hazard estimates", *Bulletin of the Seismological Society of America,* 75(4), 939-964.